

Steady-state entanglement of spatially separated qubits via quantum bath engineering

Camille Aron,¹ Manas Kulkarni,¹ and Hakan E. Türeci¹

¹*Department of Electrical Engineering, Princeton University, Princeton, NJ 08544, USA*

We propose a scheme for driving a dimer of spatially separated qubits into a maximally entangled non-equilibrium steady state. A photon-mediated retarded interaction between the qubits is realized by coupling them to two tunnel-coupled leaky cavities and each cavity is driven by a microwave drive. The proposed cooling mechanism relies on striking the right balance between Hamiltonian dynamics, the *fluctuations* of the photon fields, the *dissipative* qubit decay and the photon leakage. After mapping the dimer to an effective transverse-field XY model in a non-equilibrium bath, we show that both singlet and triplet states can be obtained with remarkable fidelities. We derive analytical expressions for these fidelities in the non-equilibrium steady state. The proposed protocol can be implemented with a superconducting circuit architecture that was recently experimentally realized, and paves the way to achieve large-scale entangled systems.

Introduction. The preparation of stable entangled states is critical to envision large-scale quantum computation and simulation schemes [1]. A particularly promising route to engineering long-lived and pure entangled quantum many-body states employs quantum bath engineering [2–4]. From this perspective, hybrid light-matter systems, particularly those realized on superconducting circuits, represent a unique platform because they offer a vast number of experimentally tunable parameters, aiding in engineering both the underlying Hamiltonian and the quantum baths to optimally drive a quantum system to a stable non-equilibrium steady state (NESS) [5]. A method of quantum bath engineering that is versatile and effective is cavity-assisted cooling which has been investigated in the context of atomic gases [6–10], optomechanical [11, 12] and spin systems [13]. In the context of superconducting qubits, a recent proposal [14] involved tailoring the photon shot-noise spectrum to cool a single qubit to any target state on the Bloch sphere. Concomitantly, remarkable experimental progress in preparing entangled states was made with superconducting qubits [15–18] and trapped ions [19], and there has been interesting related theoretical proposals [20–25]. Several challenges however remain for achieving higher fidelities and scaling up these systems to many-body entangled states.

Here, we propose and theoretically analyze an experimentally straightforward and robust scheme that builds on the cavity-assisted cooling setup employed in Ref. [14] in order to drive a spatially separated qubit-dimer into a target two-qubit state. In contrast to Refs. [16, 17], the proposed scheme only involves one microwave drive per cavity (see Fig. 1), and should be scalable to larger qubit clusters. Furthermore, the Jaynes-Cummings dimer setup that underlies the dissipative entanglement scheme proposed here has recently been experimentally realized [26] to study a dissipation driven dynamical localization transition proposed in [27]. We show that, with a suitable protocol that only involves continuous-wave drives, the system can autonomously relax to a target entangled non-equilibrium steady state, singlet or triplet, with re-

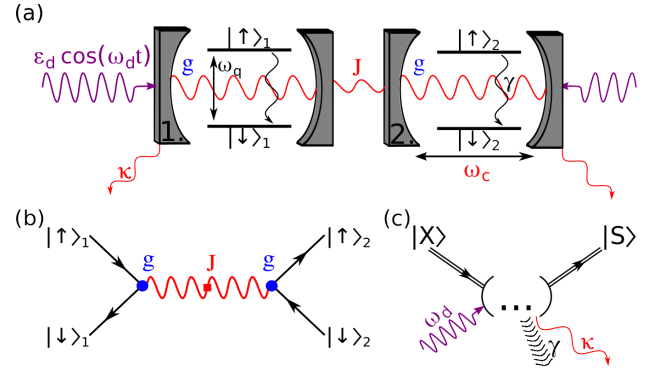


FIG. 1: (a) Two coupled cavity-qubits driven by microwave lasers. (b) Effective qubit-qubit interaction mediated by the photons. (c) NESS diagram of the cooling process from any state $|X\rangle$ to the singlet $|S\rangle$. The ellipsis symbolize the transient dynamics. The by-products are heat and photon leakage.

markably high fidelities. The mechanism relies on striking the right balance between Hamiltonian dynamics, the *fluctuations* of the photon fields, the *dissipative* qubit decay and the photon leakage. In particular, it involves optimally choosing a drive frequency ω_d commensurate with a non-trivial emergent energy scale of the open circuit-QED dimer.

We first introduce the driven circuit-QED dimer system [26, 27] as well as the typical experimental values of various parameters. Integrating out the photonic subsystem we arrive at an effective transverse-field XY model with cavity-mediated retarded interactions that can be described by a suitably secularized Master equation. After characterizing the emergent energetics of the system, we describe the different protocols to cool it to desired entangled states and compute the corresponding fidelities. Those can be measured via readily available two-qubit quantum-state tomography measurements [16]. We shall also discuss our findings in the broader context of many-body driven dissipative quantum systems.

Model. We consider a set of two identical two-level systems (“qubits”) embedded in two identical single-

mode cavities which can exchange photons, as shown in Fig. 1. Both cavities are driven out of equilibrium by two identical coherent drives which are detuned from the cavity frequency. We consider the following Hamiltonian

$$H = H_\sigma + H_{\sigma,a} + H_a + H_{\sigma,b} + H_b, \quad (1)$$

with H_σ , $H_{\sigma,a}$, and H_a respectively the qubit, the light-matter coupling, and the photon Hamiltonians (we set $\hbar = 1$)

$$H_\sigma = \sum_{i=1}^2 \omega_q \frac{\sigma_i^z}{2}, \quad H_{\sigma,a} = g \sum_i \left[a_i^\dagger \sigma_i^- + a_i \sigma_i^+ \right], \quad (2)$$

$$H_a = \sum_i \left[\omega_c a_i^\dagger a_i + 2\epsilon_d \cos(\omega_d t) (a_i + a_i^\dagger) \right] - J \left(a_1^\dagger a_2 + a_1 a_2^\dagger \right) + H_{\text{leak}}. \quad (3)$$

The two-level systems are represented by $SU(2)$ pseudo-spin operators, namely Pauli matrices, obeying $[\sigma_i^a, \sigma_j^b] = 2i\delta_{ij}\epsilon_{abc}\sigma_i^c$ where the spin indices $a, b, c = x, y, z$, the cavity indices $i, j = 1, 2$ and $\sigma_i^\pm \equiv (\sigma_i^x \pm i\sigma_i^y)/2$. ω_q is the energy splitting between ground and excited qubit states, a_i^\dagger and a_i are respectively the cavity-photon creation and annihilation operators, $[a_i, a_j^\dagger] = \delta_{ij}$. g is the light-matter coupling constant, ω_c is the cavity frequency, and J sets the strength of the photon-hopping between both cavities. ϵ_d and ω_d are respectively the strength and the frequency of both drives. H_{leak} takes into account the photon-leakage outside the cavities which broadens the cavity density of states, $\rho_c(\omega)$, by an energy scale κ : $\rho_c(\omega) = -\text{Im } G_c^R(\omega)/\pi$ where the cavity retarded Green's function is given by $G_c^R(\omega) = 1/(\omega - \omega_c + i\kappa/2)$. H_σ alone corresponds to two independent bare qubits, the eigenstates and eigenenergies of which are given by the triplet and singlet states:

$$\begin{aligned} |T_+\rangle &\equiv |\uparrow\rangle_1 \otimes |\uparrow\rangle_2 \equiv |\uparrow\uparrow\rangle, & E_{T_+} &= \omega_q, \\ |S\rangle &\equiv [|\uparrow\downarrow\rangle - |\downarrow\uparrow\rangle]/\sqrt{2}, & E_S &= 0, \\ |T_0\rangle &\equiv [|\uparrow\downarrow\rangle + |\downarrow\uparrow\rangle]/\sqrt{2}, & E_{T_0} &= 0, \\ |T_-\rangle &\equiv |\downarrow\downarrow\rangle, & E_{T_-} &= -\omega_q. \end{aligned} \quad (4)$$

To take into account the dissipation in the qubit sector, we couple the qubits to two independent zero-temperature bosonic baths given by

$$H_{\sigma,b} = \eta \sum_{i,n} \sigma_i^x (b_{in} + b_{in}^\dagger), \quad H_b = \sum_{i,n} \omega_n b_{in}^\dagger b_{in}. \quad (5)$$

The b_{in} 's are non-interacting bosons with energies ω_n . Ultimately, the strength of the qubit decay enters the equations through the hybridization parameter $\gamma \propto \eta^2/W$ where W is the typical bandwidth of the baths. We shall see that the qubit decay plays an instrumental role in our cooling scheme. In Table I, we give the typical experimental energy scales.

$$\omega_c = 6 \quad \omega_q = 7 \quad g = 2.10^{-1} \quad J = 5.10^{-2} \quad \gamma = 5.10^{-3} \quad \kappa = 5.10^{-3}$$

TABLE I: Typical energy scales (in GHz) that we consider.

Effective dissipative XY model. We treat the light-matter coupling with a second order perturbation theory in g/Δ where $\Delta \equiv \omega_q - \omega_c$ and we eliminate the explicit time-dependence of the Hamiltonian by use of a rotating wave approximation. This can be done by first transforming the Hamiltonian in Eq. (10) with the Schrieffer-Wolff transformation, $H \mapsto U_{\text{SW}} H U_{\text{SW}}^\dagger$, where

$$U_{\text{SW}} \equiv \prod_{i=1}^2 \exp \left[\frac{g}{\Delta} (a_i \sigma_i^+ - a_i^\dagger \sigma_i^-) \right]. \quad (6)$$

Up to the order $(g/\Delta)^2$, this operation eliminates the non-linearities in $H_{\sigma,a}$ at the expense of renormalizing the qubit sector. As a consequence, the photon hopping gives rise to an effective qubit-qubit interaction, see Fig. 1 (b). We then go to a rotating frame, $H \mapsto U_{\text{rot}} [H - i\partial_t] U_{\text{rot}}^\dagger$, with

$$U_{\text{rot}} \equiv \prod_{i=1}^2 \exp \left[i\omega_d t \left(\frac{\sigma_i^z}{2} + a_i^\dagger a_i + \sum_n b_{in}^\dagger b_{in} \right) \right], \quad (7)$$

and we neglect the fast rotating terms of the form $e^{2i\omega_d t} a_i^\dagger$. In the rotating frame, the bare energies are shifted by ω_d : $\omega_q \mapsto \omega_q - \omega_d$, $\omega_c \mapsto \omega_c - \omega_d$. We further decompose the two photon fields into mean fields plus fluctuations:

$$a_i \equiv \bar{a} + d_i, \quad a_i^\dagger \equiv \bar{a}^* + d_i^\dagger, \quad \text{and } \bar{n} \equiv |\bar{a}|^2, \quad (8)$$

where (in the lowest order in the light-matter coupling)

$$\bar{a}_1 = \bar{a}_2 \equiv \bar{a} \simeq \frac{\epsilon_d}{\omega_d - \omega_c + J + i\kappa/2}. \quad (9)$$

We neglect terms that are quadratic in the d 's [14]. The mean-field photonic background renormalizes the qubit sector and results in the following Hamiltonian

$$\tilde{H} = \tilde{H}_\sigma + \tilde{H}_{\sigma,d} + \tilde{H}_d + \tilde{H}_{\sigma,b} + \tilde{H}_b. \quad (10)$$

The decoupled qubit system is now coupled due to retarded cavity mediated interaction, providing an experimental realization of a two-site transverse-field XY model:

$$\tilde{H}_\sigma = \sum_{i=1}^2 \mathbf{h} \cdot \frac{\boldsymbol{\sigma}_i}{2} - \frac{J}{2} \left(\frac{g}{\Delta} \right)^2 [\sigma_1^x \sigma_2^x + \sigma_1^y \sigma_2^y], \quad (11)$$

with $(h^x, h^y, h^z) \equiv (-\text{Re } \Omega_R, \text{Im } \Omega_R, \Delta_q)$ where $\Omega_R \equiv -2(g/\Delta)(\epsilon_d - J\bar{a})$ and $\Delta_q \equiv \omega_q - \omega_d + (g/\Delta)^2 [(2\bar{n} + 1)\Delta - 2J + 2\epsilon_d \text{Re } \bar{a}]$. The eigenstates and

eigenenergies of \tilde{H}_σ to lowest order in g/Δ are

$$\begin{aligned} |\tilde{T}_+\rangle &\simeq |T_+\rangle - \frac{\Omega_R^*}{\sqrt{2}\Delta_q} |T_0\rangle, & E_{\tilde{T}_+} &\simeq \Delta_q + \frac{|\Omega_R|^2}{2\Delta_q}, \\ |\tilde{S}\rangle &= |S\rangle, & E_{\tilde{S}} &= J(g/\Delta)^2, \\ |\tilde{T}_0\rangle &\simeq |T_0\rangle + \frac{\Omega_R|T_+\rangle - \Omega_R^*|T_-\rangle}{\sqrt{2}\Delta_q}, & E_{\tilde{T}_0} &\simeq -J(g/\Delta)^2, \\ |\tilde{T}_-\rangle &\simeq |T_-\rangle + \frac{\Omega_R}{\sqrt{2}\Delta_q} |T_0\rangle, & E_{\tilde{T}_-} &\simeq -\Delta_q - \frac{|\Omega_R|^2}{2\Delta_q}. \end{aligned} \quad (12)$$

The degeneracy between $|S\rangle$ and $|T_0\rangle$ has been lifted by the effective qubit-qubit interaction. The triplet states were modified by the light-matter interaction, however the eigenstate $|\tilde{S}\rangle$ still corresponds to the singlet state of the two bare qubits. This is ensured by our symmetric set-up in which both qubits, cavities, and drives are identical.

Photon fluctuations on top of the coherent part couple to the qubits via

$$\begin{aligned} \tilde{H}_{\sigma,d} &= \left(\frac{g}{\Delta}\right)^2 \sum_i \left[\left(\frac{\epsilon_d}{2} + \Delta\bar{a}^*\right) d_i + \text{h.c.} \right] \sigma_i^z \\ &\quad - J \left(\frac{g}{\Delta}\right) [d_1\sigma_2^+ + d_2\sigma_1^+ + \text{h.c.}] \\ &\quad - \frac{J}{2} \left(\frac{g}{\Delta}\right)^2 [\bar{a}(d_1^\dagger + d_2^\dagger) + \text{h.c.}] [\sigma_1^z + \sigma_2^z], \end{aligned} \quad (13)$$

which induces transitions between the eigenstates of \tilde{H}_σ . Up to the order $(g/\Delta)^2$, the last term in Eq. (13) commutes with \tilde{H}_σ and can therefore be discarded as it does not contribute to the dynamics. We treat $\tilde{H}_{\sigma,d}$ and $\tilde{H}_{\sigma,b}$ as perturbations to \tilde{H}_σ and access the reduced density matrix of the spin sector, ρ_σ , by integrating over the degrees of freedom of these baths *via* a Master equation approach. Importantly, as the relaxation time scale of the photon-fluctuation bath, $1/\kappa$, can be larger than the typical time scale on which ρ_σ evolves, the dynamics of the latter is *a priori* non-Markovian. However, once a steady state is reached, $\rho_\sigma^{\text{NESS}} \equiv \lim_{t \rightarrow \infty} \rho_\sigma$, the usual Markovian approximation is exact [28–30] and we obtain the following non-equilibrium steady-state Master equation

$$\begin{aligned} \partial_t \rho_\sigma^{\text{NESS}} = 0 &= -i \sum_k E_k [|k\rangle\langle k|, \rho_\sigma^{\text{NESS}}] \\ &\quad + \sum_{kl} \Gamma_{k \rightarrow l} \mathcal{D}[|l\rangle\langle k|] \rho_\sigma^{\text{NESS}}, \end{aligned} \quad (14)$$

where k and l span the eigenstates of \tilde{H}_σ (see below). The integration over the bath degrees of freedom yielded both the transition rates $\Gamma_{k \rightarrow l}$ between those states (Fermi golden rule) [31] as well as the Lamb-shift (real part of self-energy) renormalizations of the energy levels $E_k \mapsto E_k + \delta_k$ with, to the leading order, $\delta_{\tilde{T}_+} = -2\alpha^2 \text{Re}[G_c^R(E_{\tilde{T}_0} - E_{\tilde{T}_+} + \omega_d) + G_c^R(E_{\tilde{S}} - E_{\tilde{T}_+} + \omega_d)]$, $\delta_{\tilde{S}} = -2\alpha^2 \text{Re}[G_c^R(E_{\tilde{T}_-} - E_{\tilde{S}} + \omega_d)]$, $\delta_{\tilde{T}_0} = -2\alpha^2 \text{Re}[G_c^R(E_{\tilde{S}} - E_{\tilde{T}_0} + \omega_d)]$, and $\delta_{\tilde{T}_-} = 0$ where $\alpha \equiv J(g/\Delta)/\sqrt{2}$.

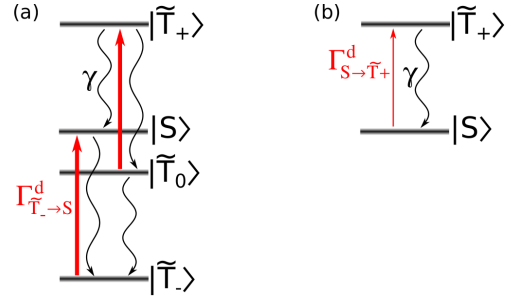


FIG. 2: Mechanism for cooling to the singlet state: (a) the photon fluctuations drive the qubit transitions from $|\tilde{T}_-\rangle$ to $|S\rangle$ and from $|\tilde{T}_0\rangle$ to $|\tilde{T}_+\rangle$ (upward arrows). (b) Once $|\tilde{T}_-\rangle$ and $|\tilde{T}_0\rangle$ are completely depleted, one is left with an effective two-level system and the dissipative channels depopulate $|\tilde{T}_+\rangle$ in favour of $|S\rangle$ (downwards arrows).

In Eq. (14), the Lindblad-type dissipators are defined as $\mathcal{D}[X]\rho \equiv (X\rho X^\dagger - X^\dagger X\rho + \text{h.c.})/2$ and the transition rates are $\Gamma_{k \rightarrow l} \equiv \Gamma_{k \rightarrow l}^d + \Gamma_{k \rightarrow l}^b$ in which the photon-fluctuation mediated part is given by

$$\Gamma_{k \rightarrow l}^d = 2 \times 2\pi |\Lambda_{kl}^d|^2 \rho_c(E_k - E_l + \omega_d). \quad (15)$$

Λ_{kl}^d and $\Gamma_{k \rightarrow l}^b$ are given by

$$\Lambda^d = \begin{pmatrix} 0 & \alpha & \alpha & 0 \\ \alpha & 0 & \beta & \alpha \\ \alpha & \beta & 0 & \alpha \\ 0 & \alpha & \alpha & 0 \end{pmatrix}, \quad \Gamma^b = \begin{pmatrix} 0 & \gamma & \gamma & 0 \\ 0 & 0 & 0 & \gamma \\ 0 & 0 & 0 & \gamma \\ 0 & 0 & 0 & 0 \end{pmatrix}, \quad (16)$$

in which rows (columns) are ordered according to $|\tilde{T}_+\rangle$, $|S\rangle$, $|\tilde{T}_0\rangle$, and $|\tilde{T}_-\rangle$ from left to right (top to bottom), and $\beta \equiv (g/\Delta)^2 [\epsilon_d(1/2 + J/\Delta_q) + \Delta\bar{a}]$. The zeroes of the lower triangular part of the Γ^b matrix in Eq. (16) arise from the zero-temperature baths that can only drain energy from the qubits.

One can re-write the Master equation (14) as the rate equations governing the population of each of the eigenstates $|k\rangle$ of \tilde{H}_σ , $n_k \equiv \langle k | \rho_\sigma | k \rangle$:

$$\frac{dn_k^{\text{NESS}}}{dt} = 0 = \sum_l n_l^{\text{NESS}} \Gamma_{l \rightarrow k} - n_k^{\text{NESS}} \Gamma_{k \rightarrow l}, \quad (17)$$

which together with the conservation law $\sum_k n_k = 1$, enables us to numerically solve for the non-equilibrium steady state.

Cooling protocols. By carefully tuning the drive frequency ω_d , one can engineer the photon fluctuations to trigger transitions from one renormalized eigenstate to another by Raman inelastic scattering. We first explain the protocol to achieve convergence to the singlet state, $\rho_\sigma^{\text{NESS}} \approx |S\rangle\langle S|$, which is governed by two time scales. The population $n_S^{\text{NESS}} \equiv \langle S | \rho_\sigma^{\text{NESS}} | S \rangle$ is a measure of the fidelity of the protocol. By choosing ω_d such that

$$\omega_d = \omega_c + E_{\tilde{S}} - E_{\tilde{T}_-}, \quad (18)$$

(note that $E_{\tilde{S}}$ and $E_{\tilde{T}_-}$ themselves depend on ω_d), the rate from $|S\rangle$ to $|\tilde{T}_-\rangle$ is $\Gamma_{\tilde{T}_-\rightarrow S}^d = J^2(g/\Delta)^2/\kappa$ and the ratio

$$\Gamma_{\tilde{T}_-\rightarrow S}/\Gamma_{S\rightarrow\tilde{T}_-} \simeq \Gamma_{\tilde{T}_-\rightarrow S}^d/\gamma \gg 1 \quad (19)$$

allows for a rapid pumping from the state $|\tilde{T}_-\rangle$ to the singlet state via Stokes (red-shifted) scattering (see Fig. 2). The particular choice of ω_d in Eq. (18) yields Lamb-shifts $\delta_{\tilde{T}_+} \simeq \delta_{\tilde{T}_0} \simeq -J/2$ and $\delta_{\tilde{S}} = \delta_{\tilde{T}_-} = 0$. Consequently, the energy splitting between the states $|\tilde{T}_-\rangle$ and $|S\rangle$ is the same as the one between $|\tilde{T}_0\rangle$ and $|\tilde{T}_+\rangle$ states [up to the order $(g/\Delta)^2$]. Therefore, $\Gamma_{\tilde{T}_0\rightarrow\tilde{T}_+}^d \simeq \Gamma_{\tilde{T}_-\rightarrow S}^d$ and there is a simultaneous pumping from $|\tilde{T}_0\rangle$ to $|\tilde{T}_+\rangle$. Both these processes are represented in Fig. 2 (a) where we did not depict the off-resonant photon-induced transitions, such as $\Gamma_{S\rightarrow\tilde{T}_+}^d$, which are sub-leading. As a consequence, the populations in states $|\tilde{T}_0\rangle$ and $|\tilde{T}_-\rangle$ are rapidly moved to $|S\rangle$ and $|\tilde{T}_+\rangle$ on a very short time scale, $1/\Gamma_{\tilde{T}_-\rightarrow S}^d$, associated with the fluctuation-driven transitions. At later times, dissipation drives the system to the singlet state according to the following mechanism. The only decay channel of the singlet, from $|S\rangle$ to $|\tilde{T}_-\rangle$, is inhibited by the rapid pumping to $|S\rangle$, see Fig. 2 (a). However, the state $|\tilde{T}_+\rangle$ has *two* decay channels: one to $|\tilde{T}_0\rangle$ which is similarly inhibited by the pumping back to $|\tilde{T}_+\rangle$, whereas the other one directly feeds $|S\rangle$. Ultimately, the qubits converge to the singlet state with high fidelity on a time scale which is set by the qubit decay, *i.e.* on the order of $1/\gamma$.

This separation of time scales in the dynamics can be used to find an analytic expression for the final non-equilibrium steady-state populations. Indeed, after the states $|\tilde{T}_-\rangle$ and $|\tilde{T}_0\rangle$ are completely depleted, the rate equations can be approximated by those of the two-level system constituted by $|S\rangle$ and $|\tilde{T}_+\rangle$. Here, the spin decay rate exceeds the pumping rate, thereby cooling the system to the singlet with high fidelity given by

$$n_S^{\text{NESS}} \simeq \frac{1}{1 + \Gamma_{\tilde{S}\rightarrow\tilde{T}_+}^d/\gamma} \approx \frac{1}{1 + 4\frac{\kappa}{\gamma}(\frac{g}{\Delta})^2}. \quad (20)$$

This expression agrees well with the results obtained by the numerical solution of the exact Master equation Eq. (14) as long as the two-level approximation is valid. Large drive strengths will result in departures from the two-level approximation since ϵ_d controls the transitions between $|S\rangle$ and $|\tilde{T}_0\rangle$ that were neglected. Eq. (20) transparently elucidates that the fidelity is the result of an intricate interplay between cavity decay, qubit dissipation and light-matter coupling, and can be made arbitrarily close to unity.

One may wonder if driving the transition between $|\tilde{T}_0\rangle$ and $|S\rangle$ would also result to cooling to the singlet. Despite the fact that the corresponding transition rates have

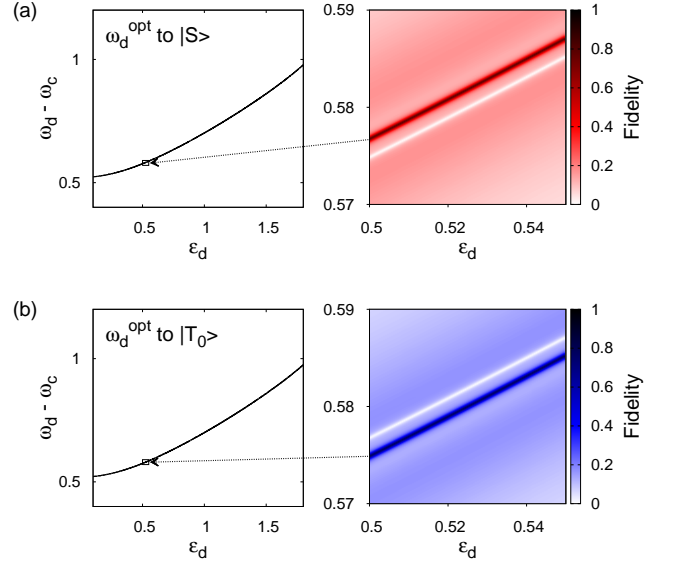


FIG. 3: (a) Cooling to $|S\rangle$. Left: optimal ω_d solution of Eqs. (18) against the drive strength ϵ_d . Right: fidelity $n_S = \langle S | \rho^{\text{NESS}} | S \rangle$ in a small region of ω_d and ϵ_d . (b) Same for cooling to $|\tilde{T}_0\rangle$. We used the parameters of Table I and units are GHz.

a prefactor $|\beta|^2$ which is of order $(g/\Delta)^4$, tuning the drive frequency $\omega_d \approx \omega_c + E_{\tilde{S}} - E_{\tilde{T}_0}$ would nevertheless result in a large ratio $\Gamma_{\tilde{T}_0\rightarrow S}^d/\Gamma_{S\rightarrow\tilde{T}_0}^d$. However, the lack of a mechanism to deplete the population of $|\tilde{T}_-\rangle$ turns it into a dark state, leading to the trivial steady state $\rho^{\text{NESS}} = |\tilde{T}_-\rangle\langle\tilde{T}_-|$.

One can also cool down the system to the other entangled eigenstate of \tilde{H}_σ , $|\tilde{T}_0\rangle$, by tuning ω_d such that

$$\omega_d = \omega_c + E_{\tilde{T}_0} - E_{\tilde{T}_-}. \quad (21)$$

The cooling mechanism is very similar to the one already described for the singlet and we shall not describe it in detail here. In practice, as the overlap between the original and the renormalized triplet states is $|\langle T_0 | \tilde{T}_0 \rangle|^2 \approx 1$, this signifies that the system can be cooled to $|T_0\rangle$ with high fidelity.

In the left panels of Fig. 3, we plot the optimal drive frequencies, solutions of Eqs. (18) and (21), to cool the system to the $|S\rangle$ and $|\tilde{T}_0\rangle$ states respectively. The difference between the optimal drive frequencies for cooling to the singlet and to the triplet state is $2J(g/\Delta)^2$. In the right panel, we present non-equilibrium steady-state ‘tomography’ of the system by representing the steady-state populations n_S^{NESS} and $n_{\tilde{T}_0}^{\text{NESS}}$ in a small region of the drive strength ϵ_d and the drive frequency ω_d . These quantities are readily measurable [16]. High fidelities can be obtained all across the parameter regime. The overall parabolic shape of the high fidelity zones stems from the quadratic dependence of the eigenenergy splittings (*e.g.* $E_{\tilde{S}} - E_{\tilde{T}_-}$) on ϵ_d . The breadth of the high fidelity zones,

the robustness of our protocol to drive parameters, can be shown to be controlled by κ^2/J .

The proposed bath engineering technique can also be used in preparing and maintaining the non-trivial $|\tilde{T}_+\rangle$ state, which corresponds to the complete inversion of the qubit populations. This is achieved by tuning ω_d such that $\omega_d = \omega_c + E_{\tilde{T}_+} - E_{\tilde{T}_-}$ in order to pump directly from $|E_{\tilde{T}_-}\rangle$ to $|E_{\tilde{T}_+}\rangle$.

In conclusion, we showed that a recently experimentally realized circuit-QED dimer system [26] can be used to engineer long-lived Bell states by optimally choosing the drive frequency to be commensurate with emergent energy scales. The proposed protocol is a solid demonstration of a situation where dissipation helps in preserving coherence [2–4].

We are grateful to Andrew Houck, Marco Schirò, Shyam Shankar, Uri Vool, and Zhen-Biao Yang for insightful discussions. This work has been supported by NSF grant DMR-115181.

-
- [1] M. A. Nielsen and I. L. Chuang, *Quantum Computation and Quantum Information* (Cambridge University Press, 2000).
 - [2] J. F. Poyatos, J. I. Cirac, and P. Zoller, Phys. Rev. Lett. **77**, 4728 (1996).
 - [3] B. Kraus, H. P. Buchler, S. Diehl, A. Kantian, A. Micheli, and P. Zoller, Phys. Rev. A **78**, 042307 (2008).
 - [4] D. Marcos, A. Tomadin, S. Diehl, and P. Rabl, New Journal of Physics **14**, 100507 (2012).
 - [5] A. A. Houck, H. E. Tureci, and J. Koch, Nat. Phys. **8**, 292 (2012).
 - [6] J. McKeever, A. Boca, A. D. Boozer, J. R. Buck, and H. J. Kimble, Rev. Mod. Phys. **73**, 565 (2001).
 - [7] V. Vuletic and S. Chu, Phys. Rev. Lett. **84**, 3787 (2000).
 - [8] P. Horak, G. Hechenblaikner, K. M. Gheri, H. Stecher, and H. Ritsch, Phys. Rev. Lett. **79**, 4974 (1997).
 - [9] D. R. Leibbrandt, J. Labaziewicz, V. Vuletic, and I. L. Chuang, Phys. Rev. Lett. **103**, 103001 (2009).
 - [10] P. Maunz, T. Puppe, I. Schuster, N. Syassen, P. W. H. Pinkse, and G. Rempe, Nature **28**, 50 (2004).
 - [11] O. Arcizet, P.-F. Cohadon, T. Briant, M. Pinard, and A. Heidmann, Nature **444**, 71 (2006).
 - [12] S. Gigan, H. R. Bohm, M. Paternostro, F. Blaser, G. Langer, J. B. Hertzberg, K. C. Schwab, D. Bauerle, M. Aspelmeyer, and A. Zeilinger, Nature **444**, 67 (2006).
 - [13] N. Brahms and D. M. Stamper-Kurn, Phys. Rev. A (R) **82**, 041804 (2010).
 - [14] K. W. Murch, U. Vool, D. Zhou, S. J. Weber, S. M. Girvin, and I. Siddiqi, Phys. Rev. Lett. **109**, 183602 (2012).
 - [15] L. DiCarlo, M. D. Reed, L. Sun, B. R. Johnson, J. M. Chow, J. M. Gambetta, L. Frunzio, S. M. Girvin, M. H. Devoret, and R. J. Schoelkopf, Nature **467**, 574 (2010).
 - [16] S. Shankar, M. Hatridge, Z. Leghtas, K. M. Sliwa, A. Narla, U. Vool, S. M. Girvin, L. Frunzio, M. Mirrahimi, and M. H. Devoret, Nature **504**, 419 (2013).
 - [17] Z. Leghtas, U. Vool, S. Shankar, M. Hatridge, S. M. Girvin, M. H. Devoret, and M. Mirrahimi, Phys. Rev. A **88**, 023849 (2013).
 - [18] N. Roch, M. E. Schwartz, F. Motzoi, C. Macklin, R. Vijay, A. W. Eddins, A. N. Korotkov, K. B. Whaley, M. Sarovar, and I. Siddiqi, arXiv:1402.1868 (2014).
 - [19] Y. Lin, J. P. Gaebler, F. Reiter, T. R. Tan, R. Bowler, A. S. Sørensen, D. Leibfried, and D. J. Wineland, Nature **504**, 415 (2013).
 - [20] F. Reiter, M. J. Kastoryano, and A. S. Sørensen, New J. Phys. **14**, 053022 (2012).
 - [21] L.-T. Shen, X.-Y. Chen, Z.-B. Yang, H.-Z. Wu, and S.-B. Zheng, Phys. Rev. A **84**, 064302 (2011).
 - [22] L. T. Shen, X. Y. Chen, Z. B. Yang, H. Z. Wu, and S. B. Zheng, Quantum Inf. Comput. **13**, 0281 (2013).
 - [23] S. Felicetti, M. Sanz, L. Lamata, G. Romero, G. Johansson, P. Delsing, and E. Solano, arXiv:1402.4451 (2014).
 - [24] S. F. Huelga, A. Rivas, and M. B. Plenio, Phys. Rev. Lett. **108**, 160402 (2012).
 - [25] A. Mezzacapo, L. Lamata, S. Filipp, and E. Solano, arXiv:1403.3652 (2014).
 - [26] J. Raftery, D. Sadri, S. Schmidt, H. E. Tureci, and A. A. Houck, arXiv:1312.2963 (2013).
 - [27] S. Schmidt, D. Gerace, A. A. Houck, G. Blatter, and H. E. Tureci, Phys. Rev. B (R) **82**, 100507 (2010).
 - [28] (The coarse-graining cell in time can be made larger than $1/\kappa$).
 - [29] H. Schoeller and G. Schon, Phys. Rev. B **50**, 18436 (1994).
 - [30] A. Mitra, I. Aleiner, and A. J. Millis, Phys. Rev. B **69**, 245302 (2004).
 - [31] A. A. Clerk, M. H. Devoret, S. M. Girvin, F. Marquardt, and R. J. Schoelkopf, Rev. Mod. Phys. **82**, 1155 (2010).